Compact phase-conjugating correlator: simulation and experimental analysis

James H. Sharp, David M. Budgett, Tim G. Slack, and Brian F. Scott

A simulation and experimental investigation of a recently proposed, compact, phase-conjugating correlator is undertaken. The effects of noise and other distortions in the input image and in the correlator filter plane are considered. As with other phase-only designs, the phase-conjugating correlator is sensitive to distortion of the input image while being robust in the presence of filter-plane distortions; this robustness is enhanced by the phase-conjugating property of the design. © 1998 Optical Society of America

OCIS codes: 070.0550, 070.5040, 070.5010.

1. Introduction

Optical correlation promises high-speed object recognition and identification for applications as diverse as target acquisition, fingerprint verification, and process and quality control. The approach proposed by Young *et al.*[1] of using a hybrid digital–optical correlator system has been adopted in this study to circumvent the performance limitations commonly imposed on correlator systems by spatial light modulator (SLM) frame rates in the input plane. However, the optical system of this proposed design employed the conventional 4*f* VanderLugt correlator, which is difficult to implement because of the need to match the phase spectra of the optically derived Fourier transform (FT) and the digitally calculated fast Fourier transform (FFT) displayed on the filter plane. This is not a trivial problem since most of the widely used SLM's, e.g., those derived from the Seiko-Epson liquid-crystal television (LCTV) projector, have a nonunity aspect ratio. Imperfections of SLM's, such as phase distortion owing to nonflatness, nonlinear phase response, residual amplitude coupling, and so on, also have implications for ultimate performance. The compact phase-conjugating correlator (PCC) devised by Duelli *et al.*[2] has been adopted to obviate some of these problems, while retaining the hybrid, high-speed concept.

A simulation of this correlator was undertaken prior to its construction to identify critical design issues and predict the effect on performance of noise and distortions. The correlator was built and tested, and its robustness to these distortions was observed experimentally.

2. Correlator Design

Figure 1 illustrates the digital and optical subsystems that constitute the correlator. Phase images of the reference data are calculated by the digital FFT system and recorded in the optical memory. This FFT system employs a Sharp Model LH9124 FFT digital signal processor chip set and can calculate a 512 × 512 FFT in less than 40 ms. Phase information is extracted from the fully complex FFT result by a GEC Plessey Pythagoras chip. Phase images are displayed at 25 Hz by use of a SLM derived from a Seiko-Epson LCTV and stored as angle-multiplexed volume holograms in crystals of Fe: $LiNbO_3$.[3] The phase conjugates of the stored images are reconstructed by use of a beam counterpropagating with respect to the reference beam, compensating for the nonunity aspect ratio and phase distortions present in the object-beam optical path. Angular translation of the reconstruction beam is achieved by use of an Isomet Model LS-110 acousto-optic deflector that provides random access to any template in the optical memory within 15 μs.[4]

The inverse transform is produced behind the SLM

When this study was performed, the authors were with the Laser and Optical Systems Engineering Centre, Department of Mechanical Engineering, James Watt Building, University of Glasgow, Glasgow G12 8QQ, UK. D. M. Budgett is now with the Department of Engineering Science, University of Auckland, Private Bag 92019, Auckland, New Zealand. T. G. Slack is now with Sowerby Research Centre, Department of Optics and Laser Technology, FPC 267, P.O. Box 5, Bristol BS12 7QW, UK.

Received 5 January 1998; revised manuscript received 10 April 1998.

0003-6935/98/204380-09$15.00/0

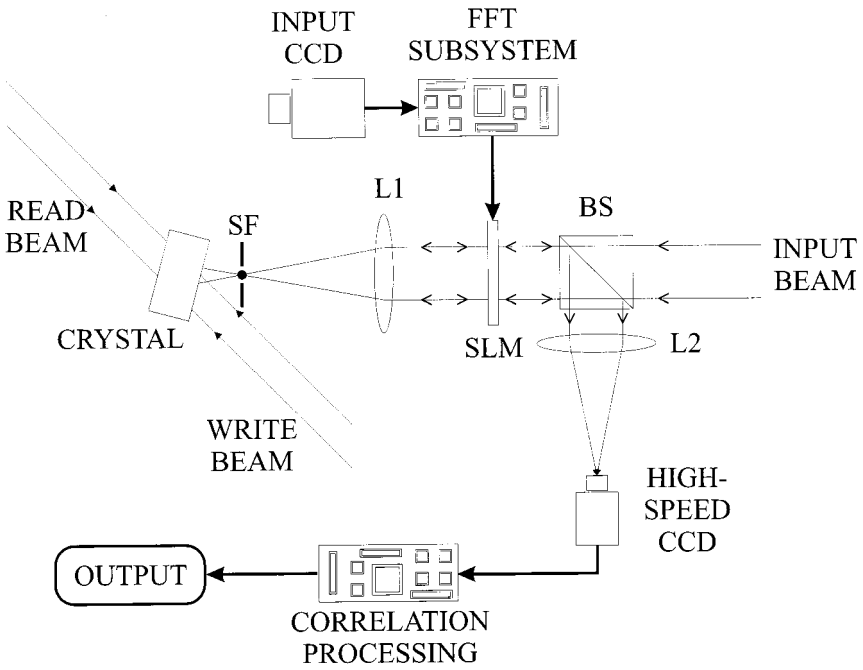

Fig. 1. Correlator design: SF, spatial filter and point stop; L, lens; BS, beam splitter.

and is extracted and scaled by use of a beam-splitter and lens system, with images of the correlation plane being captured and digitized to analyze correlation-peak characteristics. A high-speed, area-scan CCD camera captures the correlation-plane data and passes them to a specially built imaging board, which implements a parallel pixel-processing architecture to characterize the correlation-plane image and the quality of any peak detected.[5] This subsystem is capable of operating at frame rates of up to 3000 frames/s, which ultimately limits the obtainable correlator speed. The system was tested with images of a camshaft bearing cap supplied by Rover, UK. An image of the object at 0° in-plane rotation is shown in Fig. 2.

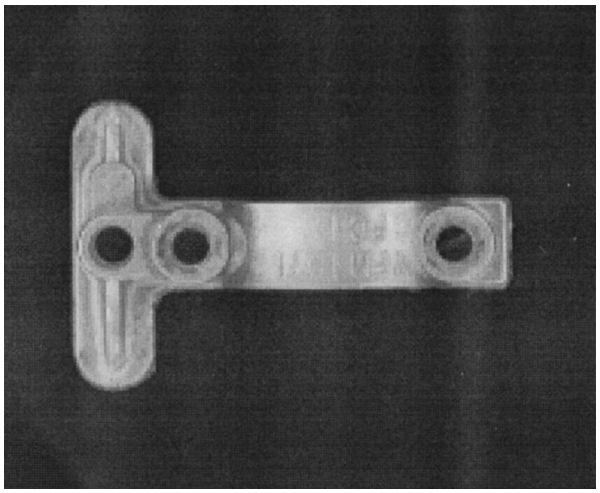

Fig. 2. Image of the test component in the reference position of a 0° in-plane rotation angle.

3. Correlator Analysis

The aim is to understand the effects of any imperfections in correlator components and their impact on system performance. The effects of imperfections in the input image and in the behavior of the phase-modulating filter-plane SLM were analysed: the effects of distortions and noise, first in the input space-domain image (prior to its transformation and storage) and second in the frequency-domain phase image (as displayed on the SLM) were evaluated.

A. Input Image

1. Intensity Noise

Intensity noise present in the input image and passed to the FFT subsystem was assumed to be additive. A series of simulations was run under the assumption of a Gaussian noise distribution normalized to the maximum available gray level (255) in the input image. Values exceeding this maximum or less than the minimum gray level were set to 255 or 0, respectively. Images with increasing levels of noise degradation were derived from a reference image of the test object oriented at a 0° in-plane rotation. The simulation numerically cross-correlated these images with the original reference. The noisy image set was then applied to the PCC, and the correlation plane output was examined experimentally.

Figure 3 illustrates the quality of the autocorrelation peak, as derived from the experiment. Figure 4 shows the results of the simulation and the experiment. The same functional trend is present in both sets of data. A large reduction in the correlation-peak height (CPH) is caused by relatively small amounts of intensity noise. Because the frequency

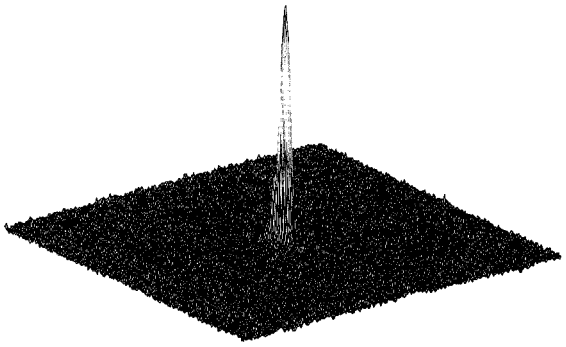

Fig. 3. Isometric plot of the experimental autocorrelation.

spectrum of the noise signal is inherently biased toward higher frequencies, minor additions of noise in the space-domain images shift a disproportionate amount of energy from the lower to the higher spatial frequencies. The pure-phase nature of the correlation exacerbates this tendency and results in the sharp drop-off observed in CPH. The performance of the PCC falls off more quickly than is predicted by the simulation. At noise levels with a standard deviation of $\sigma > 0.25$, signal levels become indistinguishable from the background-noise level in the correlation plane. To account for the experimental behavior it should be borne in mind that other imperfections, including phase errors, occur in the physical correlator, whereas the simulation examines the contribution of intensity noise in isolation.

2. *Scale and Rotation*

Pure-phase correlators are sensitive to variances in scale and rotation. The results of a simulation of the scale sensitivity of the PCC are presented in Fig. 5. Here the height of the correlation peak is plotted as a function of the percent scale error. The curve is asymmetric about the zero point because negatively scaled images result in a reduction of the total energy available to form the correlation-signal plane. However, it was found that the experimental sensitivity to scale error is more pronounced. As can be seen from Fig. 6, a +5% scale error causes a reduction of the CPH to approximately 10% of the original autocorrelation-peak height compared with the 50% reduction predicted by simulation, while a −5% scale error causes the peak to drop to 6% of its original value. This higher sensitivity is likely to be due to the spatial nonuniformity of the phase response over the aperture of the SLM area. It has been demonstrated that the application of a given gray level (i.e., a given voltage) to the SLM produces a varying phase modulation, depending on the pixel location.

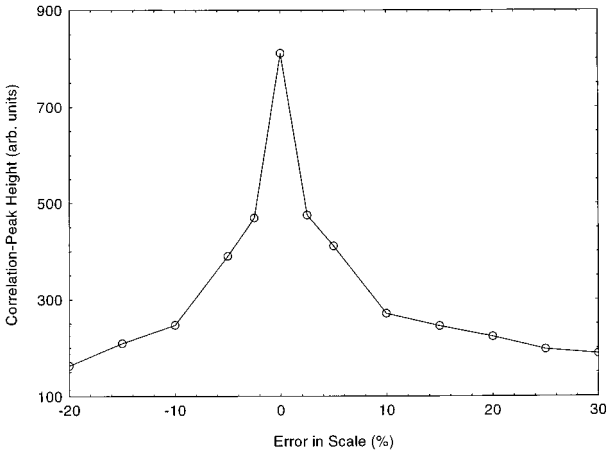

Fig. 5. Dependence of the calculated CPH on the scaling error.

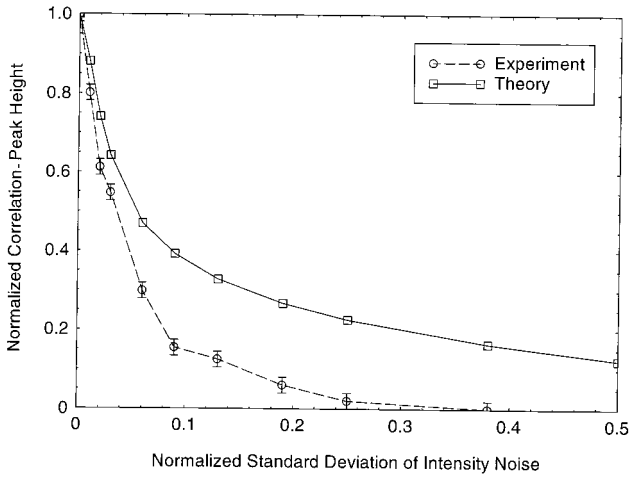

Fig. 4. Variation of the CPH with the intensity noise in the input scene.

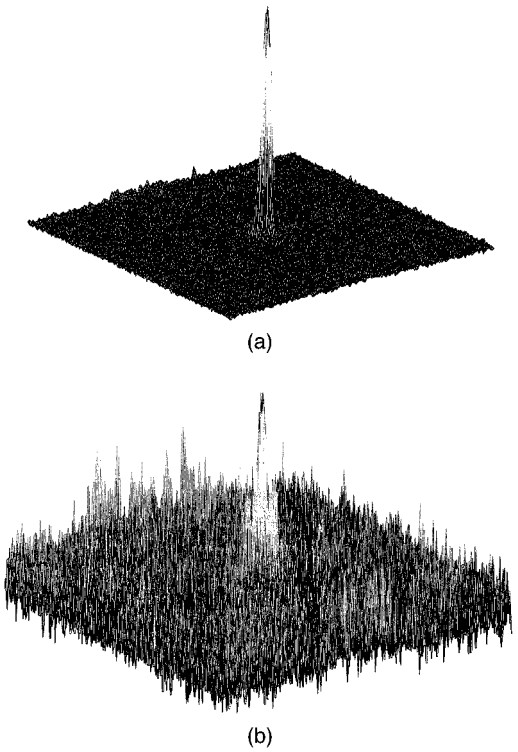

Fig. 6. Isometric plot of the experimental (a) autocorrelation and (b) cross correlation with a 5% scale increase (10× scale).

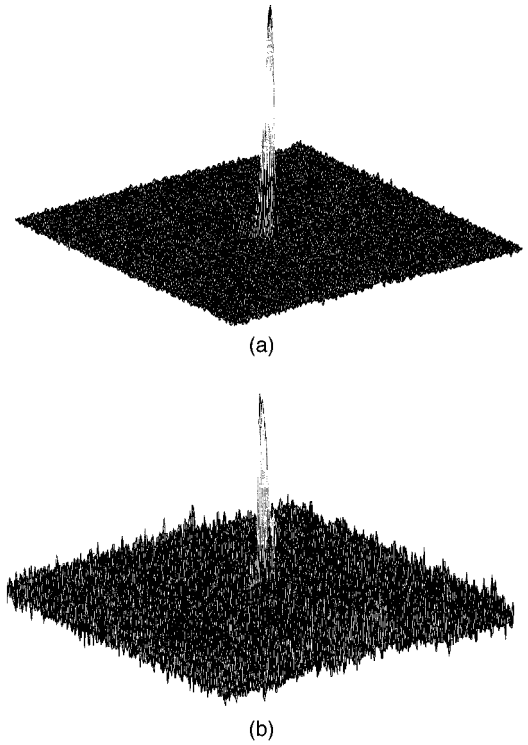

Fig. 7. Isometric plot of the experimental (a) autocorrelation and (b) cross correlation for a 1° rotation of the test component (4× scale).

An experimental cross correlation of the component rotated by 1° in plane had a similarly marked effect: As can be seen from Fig. 7, experimentally the CPH dropped to approximately 25% of the autocorrelation value, whereas a 5° rotation resulted in the CPH being reduced to 5%, just above the experimental noise background. This high degree of sensitivity to rotation might be a consequence of scaling differences in the x and y directions that results from the nonunity aspect ratio of the SLM. For these reasons, experimental verification of the simulated results below were restricted to examining the behavior of the autocorrelation function.

3. Translation

The reference image of the test component was subjected to a series of diagonal translations (e.g., 5 pixels both horizontally and vertically), and the resulting images were used to simulate the effects of translations of the object in the input plane. The simulations showed a small linear drop in the CPH caused by translations of the object. Cross correlation of the translated image set with the original was then performed by use of the PCC; the results are shown in Fig. 8. Within the experimental error, the change in the CPH with translation is linear, although it is worth noting that the rate of change is larger than that predicted by simulation. This could also be accounted for by the nonuniformity in the SLM phase response because object translation should result in a linear phase shift in the filter-plane image.

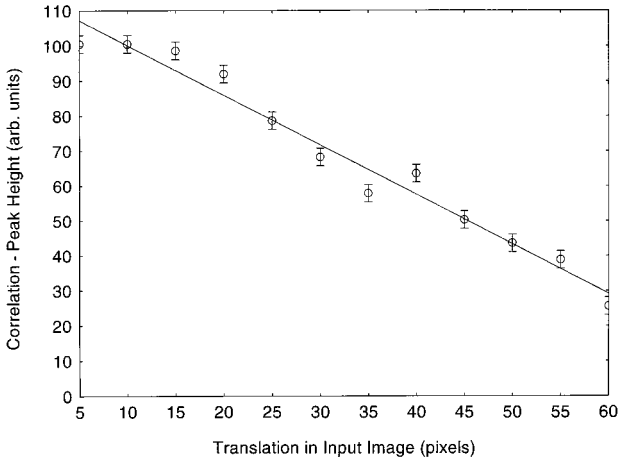

Fig. 8. Dependence of the CPH on the translation of the image in the input plane.

B. Fourier Plane

1. Lateral Misalignment

Initial alignment of the correlator optics is automatic because we are using a phase-conjugating configuration for the correlator. However, mechanical creep in the optical mounts can cause a gradual misalignment of the reconstructed phase-conjugate image with respect to the digitally calculated image displayed on the filter-plane SLM. Numerical simulations of the correlator sensitivity to misalignment are represented in Fig. 9 for the autocorrelation function. These are illustrative results, as the horizontal, vertical, and diagonal dependencies are image specific (except for the special case of circularly symmetric FT's). Step sizes of less than one pixel could be realized because the digital representation of the phase image was expanded to include three zero-amplitude pixels surrounding each image pixel. In this way the effect of the dead space surrounding pixels could be modeled, and a misalignment step size of one quarter of a pixel could be simulated.

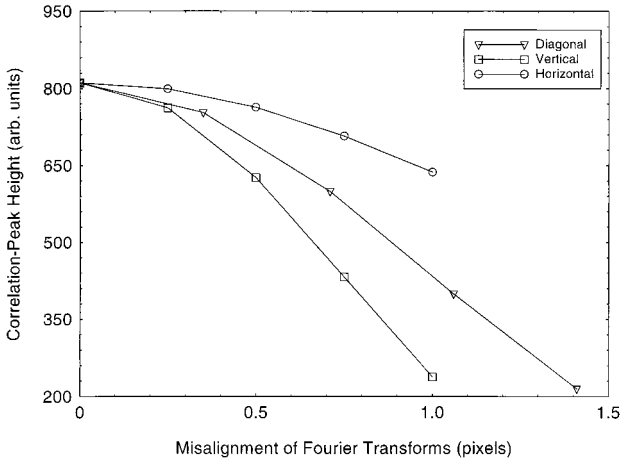

Fig. 9. Calculated dependence of the CPH on the misalignment of the reconstructed FT and SLM.

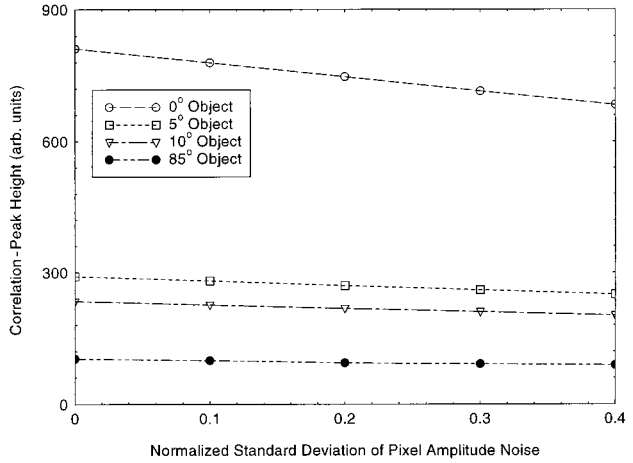

Fig. 10. Calculated dependence of the CPH on the pixel amplitude noise.

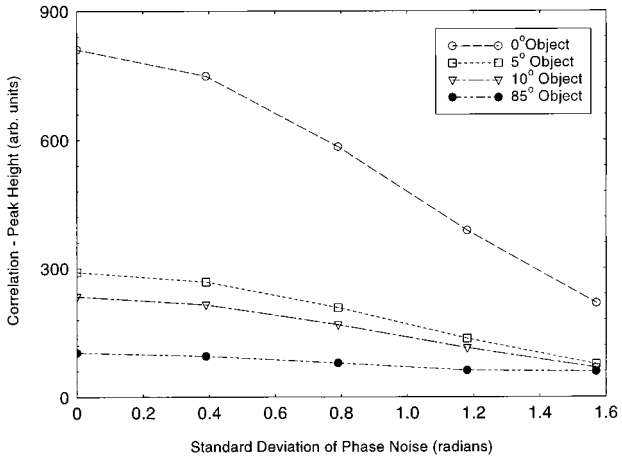

Fig. 11. Calculated dependence of the CPH on the SLM phase noise.

It is evident from Fig. 9 that a displacement of one pixel horizontally is sufficient to reduce the autocorrelation-peak height by 21%. Similar displacements vertically and diagonally produce reductions in the peak height of 71% and 51%, respectively. Experimentally it was found that a horizontal displacement of 80 μm (approximately a one-pixel pitch) reduced the autocorrelation-peak height by 64%, whereas a vertical translation of only 50 μm was enough to reduce the signal by 72%. It is apparent that lateral alignment of the phase images during reconstruction should be maintained to better than one quarter of a pixel (approximately 20 μm) to maintain the optimum correlator performance.

2. *Pixel Amplitude Noise*

A perfect phase-modulating SLM would have unity transmission for every pixel over the full range of the phase modulation, i.e., from 0–2π. In real devices when displaying phase images, amplitude modulation of the light can occur accompanying the phase modulation.[6] This can be regarded as coupled amplitude noise: noise affecting the magnitude of the pixel phasor in the Fourier plane but leaving the phase angle unchanged. As there is no information available on the strength of this coupling prior to the simulation, the initial model employed a stochastic relation. The results of this modeling are shown in Fig. 10. Amplitude noise causes a linear decrease in the CPH. At the maximum noise value, the peaks for each object have fallen to approximately 85% of their original values. Note that also shown in Fig. 9 are the simulated results for cross correlation with the images of the test object subjected to 5°, 10°, and 85° in-plane rotations.

The simulation was repeated with the addition of constant phase noise (see below) that had a standard deviation σ of 0.79 rad. The purpose of this added noise was to discover whether the correlation output would be affected by the coupling of phase and amplitude noise. It was concluded that the addition of pixel phase noise acts to lower the absolute height of the CPH but, from analysis of the correlation-plane images, does not add significantly to the noise background in the correlation plane.

This simulation could not be validated in the physical correlator because fully complex modulation would be required in the filter plane. If the pixel amplitude-coupling response is uniform over the SLM, this effect will be compensated by the phase-conjugating property of the correlator. A nonuniform response might be expected in a real SLM. However, even with the most severe noise-degradation level simulated, a relatively small decrease in the CPH of 15% occurs. Previous researchers have shown that only weak coupling might be expected in real devices.[7]

3. *Phase Noise*

The conversion of the intrinsically digital representation of the data output from the FFT system to an analog signal resampled by the SLM driver includes several opportunities for the introduction of noise. Thus the phase modulation produced in a given pixel can depart from that in the FFT phase image. The phase response is also assumed to be linear, with increasing gray levels in the filter image. This characteristic is only approximated in real devices.[8] A series of simulations was therefore undertaken to study the ways in which phase noise might affect the performance of the correlator and the implications of compounding phase noise with additional effects.

Figure 11 demonstrates the simulation of pure phase noise in affecting the autocorrelation function and some cross correlations. The correlation signals fall relatively slowly at first, but the rate of fall increases for noise levels above σ = 0.39 rad. The signals for the 0°, 5°, and 10° objects fall to 26%–29% of their original, noise-free values. This implies that the capacity of the correlation process to discriminate these objects is unaffected by the noise. However, the CPH for the 85° object falls to 57% of its original value. Thus the discrimination ratio for this object is more than halved. This difference in behavior for

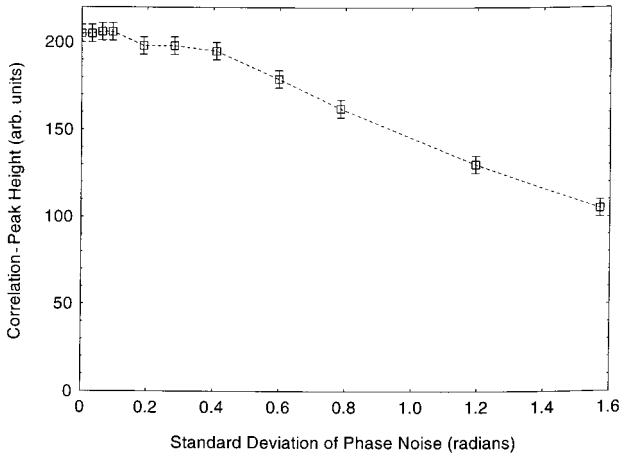

Fig. 12. Experimental dependence of the CPH on the SLM phase noise.

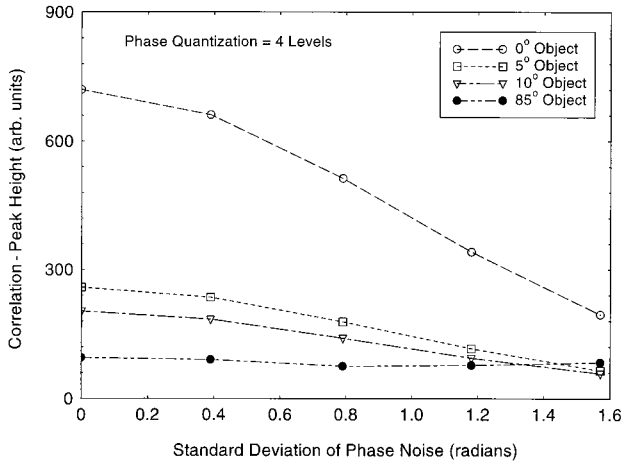

Fig. 13. Calculated dependence of the CPH on the SLM phase noise with phase quantization added.

the 85° object is explained by the closeness of the peak height compared with the noise floor of the correlation plane. As the phase noise increases, this peak collapses into the noise floor. Analysis of the correlation plane confirmed this to be the case: the location of the detected peak moved to positions remote from the original peak for tests with noise levels of $\sigma = 1.18$ rad and $\sigma = 1.57$ rad. The peaks for the 0°, 5°, and 10° objects remained in the same place for all levels of phase noise.

All four correlation peaks fell to within 92% of their noise-free values when the phase noise was 0.39 rad. At this noise level, the correlation continues to discriminate between the 0° object and any of the other objects.

For the purpose of experimental validation phase noise was added artificially to the filter-plane images. Results for the autocorrelation function are shown in Fig. 12. The functional form of the response is similar to that predicted, but, with a slightly slower falloff in the CPH with increasing noise, the total reduction in the CPH is approximately 50% at the maximum noise level. This result implies that the PCC is more robust than the simulation predicts. No increase in background noise was observed that was large enough to account for this signal level. Images captured in the correlation plane displayed a consistent level of background noise that was equivalent to ± 10 gray levels. It can be speculated that the nonlinear, nonuniform response of the SLM device reduces the amount of phase noise applied at the filter plane.

Simulations of phase noise were repeated with a fixed level of pixel amplitude noise (SLM amplitude coupling). The results were similar to those produced with pure-phase noise, although the correlation peaks were reduced in height by the additional amplitude noise. The peaks for the 0° and the 5° cases fell to 26% of their starting values; the peak produced by the 85° object fell to 54% of its initial value. However, the peak for the 10° object fell to 33%, which in turn reduced its discrimination ratio compared with the other two objects. At a phase noise level of $\sigma = 1.57$ rad together with a pixel amplitude noise of $\sigma = 0.2$, the 10° and the 5° objects produced the same CPH and could not be discriminated. However, at this noise level the output peaks of the 5° and the 10° objects shifted their locations, suggesting that correlation peaks were hidden in the noise floor. The correlation peak for the 85° object randomly changed its location at a phase noise level of $\sigma = 0.39$ rad.

The effect of phase noise in the presence of phase quantization was then considered. It was assumed that the SLM was able to display only four levels of phase (see below) with additional phase noise added as before. Figure 13 demonstrates the simulation.

Again, these results (Fig. 13) are similar to those produced for pure-phase noise, except that the peak for the 85° object does not fall as far. At the highest noise level, the signals from the 5° and the 10° objects fall below that of the 85° object. This would mean that the correlator, although able to separate the 0° object from any of the others, would not, by use of their cross-correlation values, be able to discriminate among the 5°, the 10°, or the 85° objects. This outcome was due to the presence of noise spikes in the correlation plane that become higher in the case of the 85° image than either the noise or the signals in the other correlation planes.

Experimental results are presented in Fig. 14. The functional behavior of the curve is seen to be consistent with predictions from the simulation with the reduction in the CPH for the autocorrelation function to approximately 60% of its original value. Compared with the case for phase noise only, a much larger effect is seen because the starting height of the curve is dropped owing to the additional phase quantization, whereas values at higher noise levels seem to be affected to a lesser degree. Once again, better performance is found from the experiment than might be predicted, with the correlation peak at all times clearly distinguishable from the background.

The effects of phase noise with the addition of a

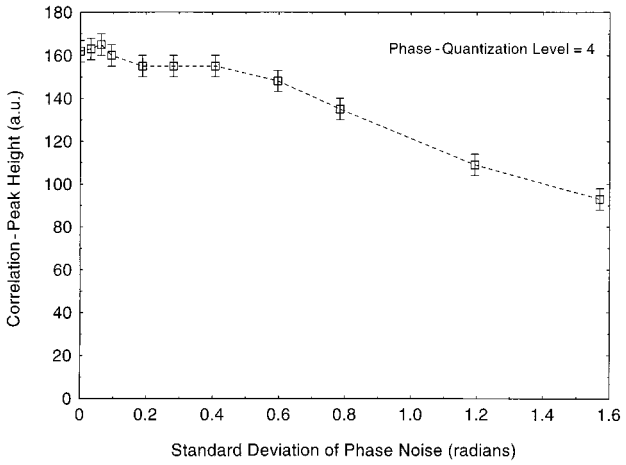

Fig. 14. Experimental dependence of the CPH on the SLM phase noise with phase quantization added.

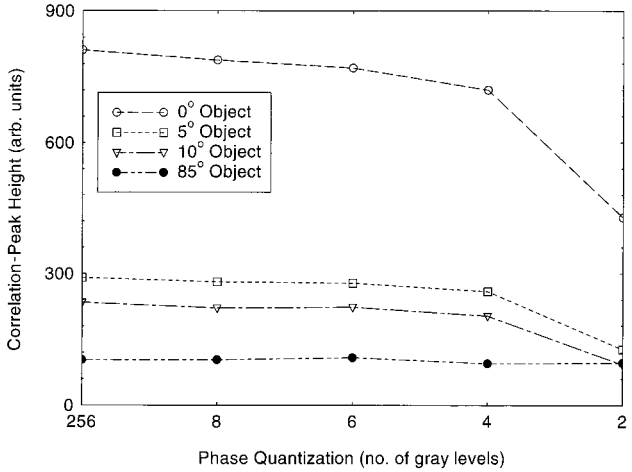

Fig. 16. Calculated dependence of the CPH on the SLM phase quantization.

constant intensity noise in the input image with a normalized standard deviation of $\sigma = 0.03$ was then considered. Results of the simulation were very similar to those found with pure-phase noise, with the effect of the intensity noise being to reduce the overall CPH across the phase noise range. As can be seen from the experimental results of Fig. 15, the autocorrelation function falls to approximately 40% of its starting value at the most extreme level of phase noise, compared with the case of phase noise alone, which produces a reduction to approximately 55% of the autocorrelation CPH (Fig. 9).

4. *Quantization*

In the attempt to increase correlator speed, binary phase-modulating SLM's have gained some acceptance, and we decided to examine the effects on correlator performance of differing levels of phase quantization. Beginning with a standard 8-bit image of 256 gray levels, we found that the number of available gray levels was reduced for the phase image and for simulations made of the comparative correlator performance. Figure 16 shows the correlation results when phase quantization was applied to the SLM in the absence of any other effects.

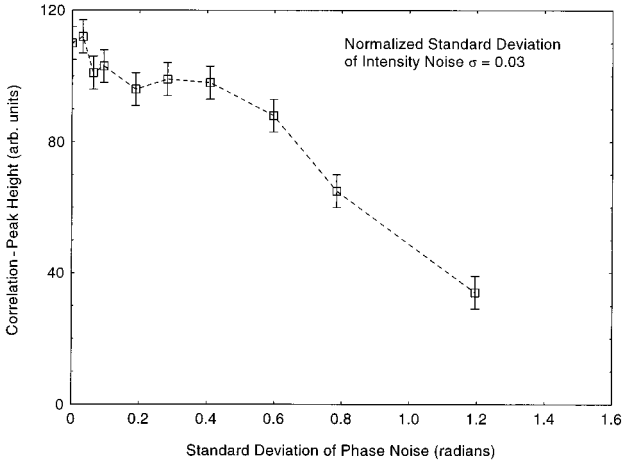

Fig. 15. Experimental dependence of the CPH on the SLM phase noise with intensity noise in the input image added.

From the simulations it was found that going from no phase quantization (32 bits of phase modulation corresponding to 2^{32} levels of phase) to a representation of the FT with just four phase levels caused only a slight reduction in the CPH. The signals for the 0°, 5°, 10°, and 85° objects fell to 89%, 89%, 87%, and 93%, respectively, of their initial values. Hence the ability of the PCC to discriminate among all three objects remained roughly constant to this level of quantization. In going to a binary phase-only filter (BPOF) representation, however, there were further dramatic falls in the peak heights for the 0°, 5°, and 10° objects of 41%, 51%, and 55%, respectively. The peak height for the 85° object remained unchanged in height but jumped to a new location, suggesting that the correlation plane consists mainly of noise spikes. A second effect seen is a relatively large variation in the CPH as the object is translated in the input image. Both these effects arise because the BPOF contains representations of both the original object and a second version rotated by 180°.[9] Both these stored objects have the same amplitude, but their phases are opposite ($-\pi/2$ and $+\pi/2$, respectively). For some positions of the input object, the cross correlation from the stored, rotated object cancels some of the main correlation peak, reducing its height.

Experimentally, the results shown in Fig. 17 were obtained. For the autocorrelation function it can be seen that an approximate decrease of 75% in the CPH is found when moving from 256 gray levels to the case of a BPOF. This result is worse than the simulation predicts when considering phase quantization in isolation from other noise and distortions, but one must recall that other sources of SLM noise are always present within this experiment.

The phase-quantization experiments were repeated in the presence of fixed levels of phase noise. The results, in terms of the percent changes in the PCH's, were almost identical to those produced by

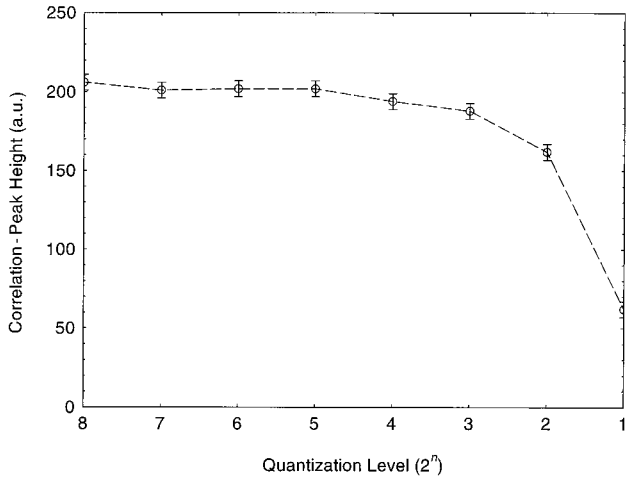

Fig. 17. Experimental dependence of the CPH on the SLM phase quantization.

quantization alone. The most significant effect was a small decrease in the initial value of the CPH for the autocorrelation function.

4. Conclusions

For noise or distortion in the input image the CPH is most sensitive to scale and rotation variance (as may be expected) and intensity noise. These effects severely degraded the peak in the correlation plane even when present in only small amounts. Generally, simulation predicted the correlator to be more tolerant than it was found to be experimentally, particularly with respect to object rotation.

Translation of the object in the image plane showed a weak linear dependence on position during operation of the PCC. This effect has been accounted for by the nonuniformity of the SLM phase response.

In the case of errors in the correlator filter plane, the most striking impact on correlator performance comes from misalignment of the phase image reconstructed from optical memory and the phase image as displayed on the SLM. From simulation and experiment it is concluded that a tolerance of ± 20 μm should apply to maintain a reasonable level of correlation output. This has clear implications for the optomechanical design of the working correlator.

Virtually no noise was observed in the correlation plane when pixel amplitude noise on the SLM was considered, even when noise levels became excessive. The intensities of the correlation peaks fall in a linear fashion as the standard deviation of the Gaussian noise increases. No changes in the discrimination of the correlation process are observed; hence the ability of the correlator to distinguish between the reference object and rotated versions of the object is unimpaired. This is an encouraging result, as the noise levels used in the simulation were higher than those expected in real devices. A repeat of the pixel amplitude-noise experiments in the presence of a fixed level of pixel phase noise yielded identical results. It is not anticipated that SLM pixel amplitude noise will pose a problem for the correlator.

Pixel phase noise was investigated by simulation and experiment in which phase noise was added artificially to test correlator tolerance. Phase noise was seen to have two main effects on the correlation process: first reduction in the PCH's and second redistribution of the light from these peaks into noise background in the correlation plane. As noise levels increase, the correlation peaks subside into an increasing noise floor. Eventually a point is reached at which the highest peak in the correlation plane is a noise spike. The result was that relatively low correlation peaks from objects quite dissimilar from the reference object quickly reached this noise floor, after which no further reduction occurred.

The effects of varying the phase noise were also investigated in the presence of fixed levels of pixel amplitude noise, phase quantization, and input-intensity noise. In these cases, the effects of phase noise were found to be nearly identical in form to those experienced from phase noise on its own, indicating little or no coupling between these effects.

The worst noise level used was $\sigma = 1.57$ rad, which can reasonably be regarded as excessive, since the range of phase values in the FT was only $-\pi$–π rad. In this case, with the 0° object as the reference, the 0° object could always be discriminated from the other three objects. However, when other fixed distortions were also present, cross correlation with the other objects could produce ambiguous results.

Phase-quantization modeling and experiments demonstrated that virtually no degradation in correlation performance was observed even if only four levels of phase were used to represent the FT. Compared with a continuous phase representation, a drop of approximately 10% was observed in the CPH's for the four-level case. With only two levels of phase, corresponding to a BPOF, there was a drop in the peak heights of ~50%, and variation in the CPH as the object was moved around in the input image plane is produced. The results for varying the levels of phase quantization in the presence of fixed levels of phase noise were virtually identical to the case in which only quantization was included. There was no apparent interaction between the distortions. It was concluded that only a limited set of phase values needs to be displayed on the SLM for high-quality correlations to be obtained.

In light of these simulations and experiments and given the levels of noise known to be present in typical SLM's, it is apparent that, although mechanical tolerances can be maintained, hybrid PCC's will make excellent high-speed correlation systems. Current performance is limited by the speed of processing the data from the correlation plane and the speed and modulation characteristics of currently available SLM's. As this technology advances, it is to be anticipated that yet higher performance can be obtained.

This study was funded by the European Commission under the Brite–EuRam research program. The authors gratefully acknowledge valuable discus-

sions with M. Duelli, now at the Electro-Optics Research Institute, and Neil Collings of the University of Neuchatel. Thanks are due to C. Buckberry of the Applied Optics Group, Rover, UK, who supplied test components.

References

1. R. C. D. Young, C. R. Chatwin, and B. F. Scott, "High-speed hybrid optical digital correlator system," Opt. Eng. **32,** 2608–2615 (1993).
2. M. Duelli, A. R. Pourzand, N. Collings, and R. Dandliker, "Pure phase correlator with photorefractive filter memory," Opt. Lett. **22,** 87–89 (1997).
3. J. H. Sharp, D. M. Budgett, P. C. Tang, and C. R. Chatwin, "An automated recording system for page oriented volume holographic memories," Rev. Sci. Instrum. **66,** 1–4 (1995).
4. J. H. Sharp, D. M. Budgett, C. R. Chatwin, and B. F. Scott, "High-speed, acousto-optically addressed optical memory," Appl. Opt. **35,** 2399–2402 (1996).
5. D. M. Budgett, P. E. Tang, J. H. Sharp, C. R. Chatwin, R. C. D. Young, R. K. Wang, and B. F. Scott, "Parallel pixel processing using programmable gate arrays," Electron. Lett. **32,** 1557–1559 (1996).
6. A. R. Pourzand, M. Duelli, and N. Collings, "Frequency plane filter performance assessment II," BRITE-EURAM project RY1, Tech. Rep. T222, Doc. ref. RY1/TR/NCH/NC&AR&MDP961205 (European Commission, Brussels, Belgium, 1996), pp. 1–6.
7. A. R. Pourzand and N. Collings, "Detailed experiments on phase modulating SLM characteristics," BRITE-EURAM Project RY1, Tech. Rep. T213-1, Doc. ref. RY1/TR/NCH/NC&ARP950523 (European Commission, Brussels, Belgium, 1996), pp. 1–14.
8. R. D. Juday, "Correlation with a spatial light modulator having phase and amplitude cross coupling," Appl. Opt. **28,** 4865–4869 (1989).
9. T. G. Slack, "Simulation of SLM degradation," BRITE-EURAM Project RY1, Tech. Rep. T341, Doc. ref. RY1/TR/BAE/TS951020 (European Commission, Brussels, Belgium, 1995), pp. 1–60.